Journal of Civil Engineering
The Institution of Engineers, Bangladesh
Vol. CE 24, No. 2, 1996

NONLINEAR FINITE ELEMENT STUDY OF SHEAR WALL—FLOOR SLAB CONNECTIONS

Md. Shafiul Bari[1]

ABSTRACT : This paper presents the results of an analytical study of the strength and stiffness of shear wall-floor slab connections using a specially developed three dimensional nonlinear finite element program. The program incorporated 20 node isoparametric brick element with embedded steel. Concrete was modelled after the equations given by Kotsovos and steel as an elastic perfectly plastic material. The accuracy of theoretical predations was tested against results of experimental work on reinforced concrete models. A total of fifteen specimens were tested to study the effect of shear reinforcement in the slab and various load and geometrical parameters that govern the strength of the connections. The theoretical strains, deflections and failure loads were compared with the experimental values. Excellent agreement was obtained between the two values.

KEY WORDS : Shear wall, slab, stiffness, shear stress, modelling, crack, shear retention factor

INTRODUCTION

A common type of structure suitable for hotels and apartment buildings is shear wall structure. The shear walls generally run perpendicular to the length of the building and are often intersected by facade and corridor walls. Where these intersect the cross walls, they act as flanges to the cross walls. The floor slabs and shear walls together act as a rigid jointed frame in resisting gravity loads and lateral forces due to wind and earthquake. Along the line of contraflexure in the floor slabs, lateral loads cause vertical shears which like the gravity loads are also finally transmitted to the walls via the floor slab. The junction between the wall and slab is therefore a key force resisting element which is subjected to severe stress concentration. This problem has already been studied theoretically by Coull and Wong (1983) to determine the distribution of shear stresses at the junction. Schwaighofer and Collins (1977) reported one adhoc test on a pair of one-third scale reinforced concrete shear walls coupled by a slab. In a recent study, experimental as well as theoretical work have been reported on slab-wall junctions for planar and flanged shear walls by Bhatt et el (1986). The object of the present investigation is to use nonlinear finite element analysis to predict the strength and stiffness of junctions.

DETAILS OF FINITE ELEMENT PROGRAM

Element Used : The theoretical analysis was carried out using a specially written 3-D nonlinear finite element program. The element used was a 20 node isoparametric brick element. This element was chosen to consider

1 Department of Civil Engineering, BUET, Dhaka-1000

the effect of the stress components σ_x, σ_y, σ_z, τ_{xy}, τ_{zx}, τ_{zy}, and in particular the vertical shear stress components τ_{yz} and for τ_{zx}, which are vital for predicting punching failure of slab-wall junction.

Simulation of Steel Reinforcement : The stiffness of reinforcing bars in the element was included by extending into three dimensions the basic ideas of using the embedded approach given by phillips et al (1976) for two dimensional problems. In this approach, full bond is assumed between concrete and steel reinforcement. This enables the strain in the reinforcement to be calculated in terms of the corresponding strain in the element and hence the corresponding stiffness of the steel reinforcement. One advantage of this approach is that the reinforcing steel can be in its exact position without imposing any restrictions on finite element mesh choice. But the bars are restricted to lie along the local coordinate lines of the isoparametric element used in this work.

Concrete Modelling : Concrete was modelled after Kotsovos et al (1979). In this approach, the failure surface is expressed in terms of three parameters, q, r and θ where

$q = \sqrt{3}\ \sigma_{oct}$, $r = \sqrt{3}\ \tau_{oct}$, $\cos\theta = (\sigma_1 + \sigma_2 - 2\ \sigma_3) / (\sqrt{6}\, r)$

σ oct, τ_{oct} =octahedral normal and shear stresses respectively, the variable θ = defines the direction of the deviatoric component of the stresses on the octahedral plane. The failure envelope on the π plane is expressed in terms of a curve with six fold symmetry. The curve is a function of cos θ and τ_o and τ_{60} which are respectively octahedral shear stresses at $\theta = 0°$ and $\theta = 60°$. τ_o and τ_{60} are given by

$\tau_o / f'_c = 0.944\ C^{0.724}$ $\qquad$ $\tau_{60} / f'c = 0.633\ C^{0.857}$.

$C = \sigma_{oct} / f'_c + 0.05$.

f'_c = cylinder compressive strength of concrete.

Similarly, for the deformational properties, use has been made of the secant bulk (k_s) and secant shear (G_s) moduli which are expressed as follows

$K_s = \sigma_{oct} / 3\epsilon_{oct}$, $G_s = \tau_{oct} / 2\gamma_{oct}$

Extensive tests have confirmed that the model is applicable to concretes with uniaxial cylinder compressive strength varying from 15 to 60 N/mm^2. All these empirical expressions for deformational as well as strength properties of concrete were successfully implemented in the computer program and subsequently used in the present work.

Modelling of Cracking : Smeared crack approach was adopted. Cracking was monitored at 27 Gauss points in the element. After concrete cracks, it no longer remains isotropic and anisotropic yield conditions prevail. After the first crack, concrete yielding is governed by laws similar to Kupfer et al (1973) depending on the biaxial state of stress prevailing in

the plane of the crack. Concrete is assumed to fail in crushing mode in compression either due to violating the failure surfae presented above or due to reaching the principal compressive strain of 0.0035. Similarly concrete cracks if the maximum tensile principal stress is equal to 50% of the cylinder split strength. The main features of the cracking model adopted are i) cracking in one, two or three directions is allowed, ii) cracks are allowed to open or close during the load increment, iii) no tension stiffening but shear retention is allowed and iv) variable crack direction is allowed. For incorporating a realistic shear retention factor, β, to model shear transfer across cracked concrete, the following nonlinear relationship based on the average of the three principal strains at any cracked point is used

$\beta = 1.0$ if $\epsilon_m < \epsilon_{to}$

$\beta = 0.25\ \epsilon_{to} / \epsilon_m$ if $\epsilon_m \geq \epsilon_{to}$

where ϵ_m = fictitious mean principal strain

ϵ_{to} = cracking strain = 0·0001.

Method of Solution : An incremental -iterative approach was adopted. The stiffness matrix is evaluated using secant rigidity matrix. The stiffness matrices are updated only at the second iteration in each increment except for the first increment. Equilibrium is checked against the residual forces given by the difference between the total applied load on the structure and the nodal forces calculated using the stress in the elements. Iteration stops when the ratio of the square root of the sum of the squares of the residual forces to the applied forces is less than a specified tolerance. In the present work this ratio was taken as 10%. The maximum number of iterations was fixed at 20. Adopting a more accurate tolerance did not show much difference in the behaviour other than increasing the computation cost. The analysis was terminated by monitoring the growth of iterative displacements. This was coupled with a search through the diagonal terms of the stiffness matrix to detect zero or negative values, in which case the analysis was terminated.

EXPERIMENTAL WORK

The experiments were done on reinforced concrete models designed to represent the local stress state at the junction. Since the problem of the strength of a shear wall-floor slab junction under investigation was one of local stress concentration, no attempt was made to use scale models to correspond to any prototype. The main considerations were reasonable representation of the stress state in the actual structure, economy in the use of materials and ease of handling and loading, according to the capacity of the available equipment. The floor slabs were approximately one meter square and 150 mm thick. The slab was cast monolithic with a

short height of the wall. The wall was held down to the laboratory floor by two prestressing strands which passed through two holes in the wall. Using two stiff beams, the gravity load was applied as two line loads parallel to the wall web and acting at the edges to the slab. The shear force due to wind load was applied as another line load normal to the wall web and at the edge of the model. Fig 1(a) shows a typical model with loading beams and Fig 1(b) shows the loading and supporting arrangement for models under test. The models were monitored for ultimate load, mode of failure, crack development and tensile stress in the reinforcement. Table 1 shows the main dimensions of the models tested and details can be found in Reference 1.

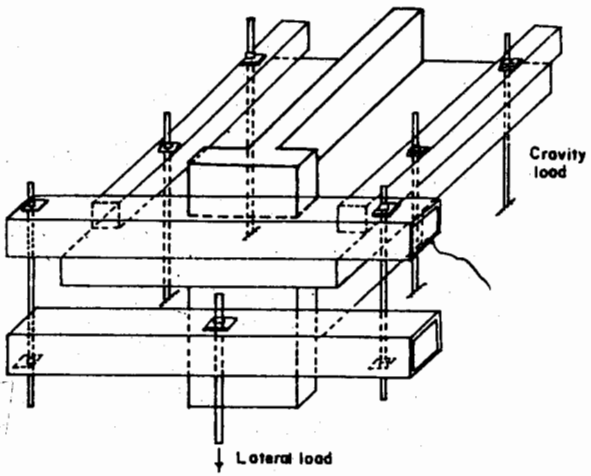

Fig 1. (a) Typical Model with Loading Beams

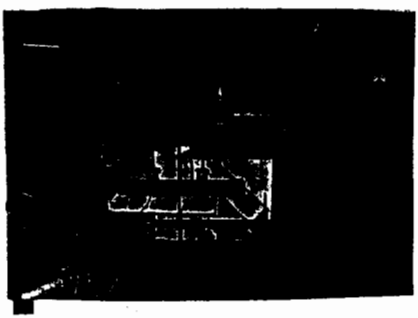

Fig 1. (b) Loading and Supporting Arrangement

Table 1. Dimensions of models in millimeters

Model No.	Wall Web	Wall flange	Wall thick ness	Slab canti lever	Slab thick ness	V_{exp} KN	V_{theo} KN	$\frac{V_{exp}}{V_{theo}}$
PS1	900	125	125	450	150	219	200	1.10
PS2	900	125	125	450	150	159	180	0.89
PS3	900	125	125	450	150	175	180	0.97
MS4	400	125	125	475	150	191	220	0.87
MS5	400	125	125	595	150	203	200	1.02
MS6	600	125	125	355	150	343	330	1.04
MS7	600	125	125	475	150	262	260	1.00
MS8	600	125	125	475	150	280	280	1.00
MS9	600	125	125	475	150	247	250	0.99
MS10	700	300	100	300	100	209	220	0.95
MS11	700	200	100	300	100	219	200	1.00
MS12	700	400	100	300	100	235	230	1.02

Note : *All the slabs had a width of 1000 mm except model MS9 which had a width of 1440 mm.*

THEORETICAL ANALYSIS

The analysis was carried out assuming zero wall thickness and eight slab elements as shown in Fig 2. Preliminary analysis had shown that inclusion of wall thickness made little difference to the final result, Fig 3. Similarly the value of shear retention factor β was varied and the 'best' correlation was obtained for the relationship given before, Fig 4. During experiment, loading was essentially displacement controlled. Especially at the initial stages, the wind shear applied using a stiff beam was such that the edged of the slab had constant displacement. However the nonlinear program could follow only force control. The procedure adopted in the numerical analysis was as follows. In the elastic state, the slab was subjected to a constant edge displacement. From this analysis not only the total wind shear was calculated but also the distribution of nodal forces due to wind shear. It was assumed that the distribution remained constant during the entire load history. Similarly gravity and lateral loads were not applied proportionately in the tests, whereas proportional loading was used in the theoretical analysis. Additional analysis indicated that the errors are unlikely to be of any significance.

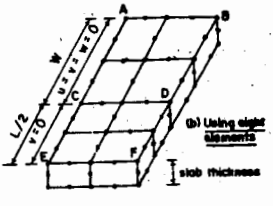

Fig 2. Finite Element Mesh with Boundary Conditions

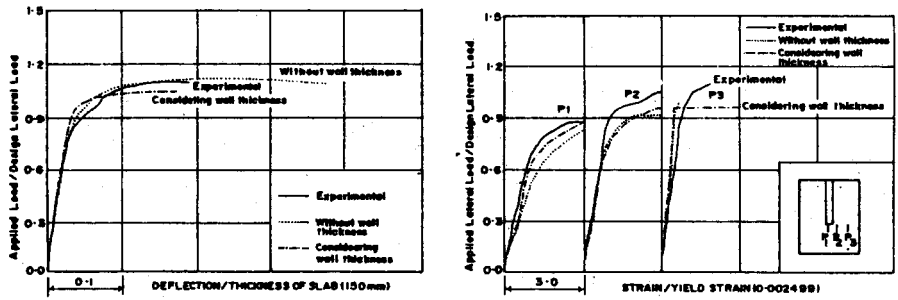

Fig 3.(a) Effect of Wall Thickness on Lateral Load Displacement Relations of Model 'MS7'; (b) Effect of Wall Thickness on Tensile Strain in Steel in Windword Direction in the Slab of Model 'MS7'

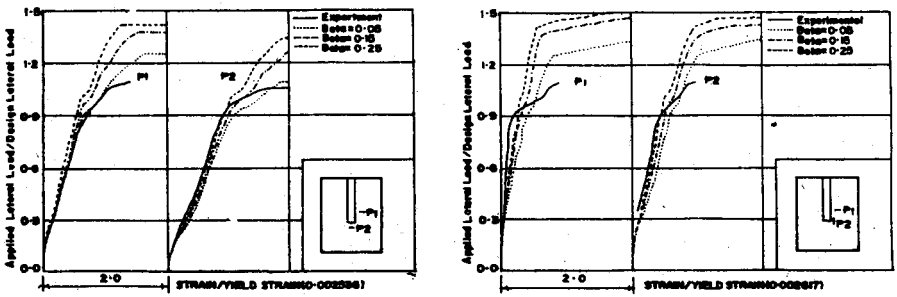

Fig 4.(a) Sheor Relation Factor, Bata, on the Tensile Strain in Steel in Transverse Direction in the Slab of Model 'MS7'; (b) Effect of Sheor Relation Factor, Beta, on the Tensile Strain in Closed Vertical Stirups in the Slab of Model 'MS7'

THEORETICAL RESULTS

To build confidence in the accuracy of the results obtained from the finite element program, the distribution of vertical shear stress τ_{zx} over the depth of slab at different loading stages is presented in Fig 5. The figure shows approximate parabolic distribution of shear stress which was as expected. To illustrate progressive redistribution of shear stresses around the connection, contours of τ_{xz} and τ_{yz} are shown in Fig 6 at different loading stages. The area around the wall nose is found to be highly stressed, which is the critical area for punching failure. For all the models tested, the theoretical ultimate load (V_{theo}) is compared with experimental ultimate load (V_{exp}) in Table 1. Figure 7 shows the comparison between the theoretical and experimental values of displacements and strains in steel and concrete.

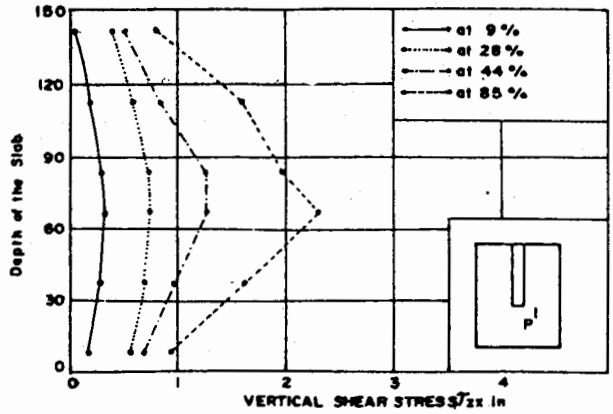

Fig 5. Variation of Vertical Shear Stress Tzx of Point Pl Along Depth of Slob of Model PSI at Different Stages of Loading

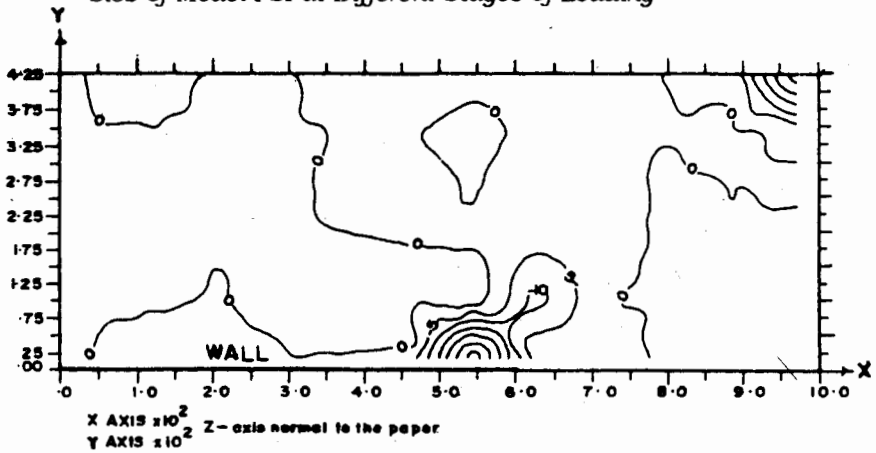

Fig 6.(a) Contour lines of Shear Stress Tzx (N/mm^2) in the Slab Model MS7 Using fixed Crack Analysis at a Lateral Load 1.04 of Design Load

CONCLUDING REMARKS

The theoretical analysis shows that the adopted modelling is eminently satisfactory in terms of predicting ultimate loads to an acceptable level of accuracy. It is interesting to note that not only the flexural type of failure was successfully predicted, but also the punching type. The mean and standard deviation for the results of ultimate load ratio (V_{exp}/V_{theo}) was 0.99 and 0.06 respectively. The analysis was able to predict correct values of the loads and strains irrespective of the mode of failure. The results for strains and displacements also show acceptable agreement between measurement and theory.

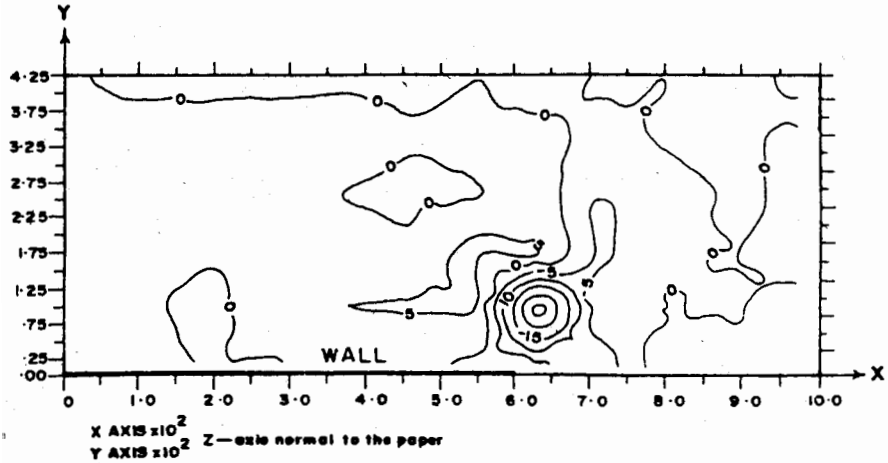

Fig 6. (b) Contour Lines of Shear Stress Tyz (N/mm²) in the Slab Model MS7 Using flexed Crack Analysis at a Lateral Load 1.04 Design Load

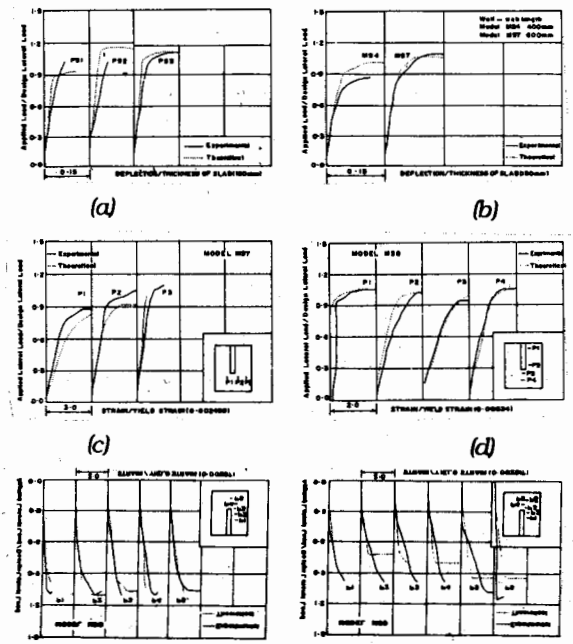

Fig 7. Lateral Load Displacement Curves for Models of Preliminary Series to Study the Effects of (a) Shear Steel; and (b) Wall Web Length; Tensile Strain in Steel in; (c) Windward Direction Along Transverse Section in the Slab of Model MS7; and (d) in Transverse Direction in the Slab Model MS8; (e) Strain in Closed Vertical Stirrup of Different Locations in the Slab of models MS8; (f) Compressive Strain in Concrete in Windward direction in the Slab of Model MS7

REFERENCES

Bari, M. S. and Bhatt, P. (1993), "Tests on shear wall-floor slab connections with shear reinforcement", Journal of the Institution of Engineers, Bangladesh, Vol. 21, No. 2, 15-28.

Bhatt, P., Memon, M. and Bari, S. (1986), "Strength of plane shear wall-floor slab junction", Proceedings of the International symposium on fundamental theory of reinforced and prestressed concrete, Nanjing, China, Vol. 3, 541-549.

Bhatt, p. and Elnounu, G. F. (1986), "Strength of flanged shear wall-floor slab junction", Proceedings of the Third International conference on computational methods and experimental measurement, Porto carras, Greece, Vol. II, 525-538.

Coull, A. and Wong, Y. C. (1983, "Design of floor slabs coupling shear walls", Journal of Structural Eng. Proceedings ASCE, Vol. 109, No. 1, 109-125.

Kotsovos, M. D. (1979), "A mathematical description of the strength properties of concrete under generalized stresses", Magazine of Concrete Research, Vol. 31, No. 108, 151-158.

Kotsovos, M. D. and Newman, J. B. (1979), "A mathematical description of the deformation behaviour of concrete under complex loading", Magazine of Concrete Research, Vol. 31, No. 107, 77-90.

Kupfer, H. B. and Gerstle, K. H. (1973), "Behaviour of concrete under biaxial stresses", Journal of Engineering Mechanics Division. ASCE, Vol. 99, No. EM4, 853-866.

Phillips, D. V. and Zienkiewicz, O. C. (1976), "Finite element nonlinear analysis of concrete structures", Proceedings of Institution of Civil Engineers (London), Part 2, 59-88.

Schwaighofer, J. and Collins, M. P. (1977), "Experimental study of the behaviour of reinforce concrete coupling slabs", ACI Journal, Proceedings Vol. 74, 123-127.